

Antifungal Activity of Clove Essential Oil-Based Nanoemulsion against Tomato Fusarium Wilt and Potential Toxicity on Male Albino Rats

Abdulmohsen Abbas Almajed¹, Ahmed Mahmoud Ismail^{1,2,3,*}, Eman Said Elshewy³, Naglaa Abd Elbaki Sallam Muhanna³, Ahlam Farouk Hamouda⁴ and Eman Yehia Khafagi³

¹Department of Arid Land Agriculture, College of Agriculture and Food Sciences, King Faisal University, P.O. Box 420, Al-Ahsa 31982, Saudi Arabia; ²Pests and Plant Diseases Unit, College of Agriculture and Food Sciences, King Faisal University, P.O. Box 420, Al-Ahsa 31982, Saudi Arabia; ³Vegetable Diseases Research Department, Plant Pathology Research Institute, Agricultural Research Center (ARC), Giza 12619, Egypt; ⁴Department of Forensic Medicine and Toxicology, Teaching Hospital, Faculty of Veterinary Medicine, Benha University, Benha 13736, Egypt

*Corresponding author's e-mail: amismail@kfu.edu.sa

Fusarium wilt caused by *Fusarium oxysporum* f. sp. *lycopersici* (*FOL*) is a serious soil-borne disease of tomato (*Lycopersicon esculentum* L.). The study aimed to prepare clove essential oil (CEO) in a nanoemulsion (CEONE) form and to evaluate its antifungal potential against *FOL* in comparison to its bulk form (CEO) using a series of *in vitro* and *in vivo* experiments. CEONE was prepared and characterized using DLS, Zeta potential, and TEM analysis. The wilt disease incidence (WDI%) and wilt disease severity (WDS%) were assessed. Enzymatic activity and biochemical changes as well as histopathological alterations were subsequently investigated. Anti-proliferative effect of CEONE on male albino rats was investigated through hematological, biochemical, and histological analyses. The prepared CEONE showed a Z-average diameter of 50.75 nm having a spherical-shaped droplet structure as confirmed by TEM imaging and showed a surface charge exceeding -37.6 mV. Laboratory results revealed that CEONE had a significant antifungal activity towards *FOL* at concentrations of 50, 100, and 200 µL/L with inhibition percentages of 44.72, 64.17, and 78.06%, respectively. Greenhouse findings showed that CEONE significantly decreased the WDI and WDS of *FOL* when applied at 200 µL/L with efficacy reaching 85.19 and 87.72%, respectively. Field experimental results indicated that the application of CEONE at 200 µL/L decreased the WDI of *FOL* to 66.67% and WDS up to 60.92 % when compared to CEO, and untreated control. Application of CEONE (100 µL/L) and CEO (1000 µL/L), significantly ($p < 0.05$) upregulated the level of PPO. Whereas, the highest concentrations of CEONE (200 µL/L) and CEO (1500 µL/L) significantly ($p < 0.05$) downregulated the level of PPO. Out of all treatments, CEONE at a concentration of 50 µL/L exhibited a significant increase in total chlorophyll, and carotenoids with values reaching 54.41 µg/g FW and 2.0 µg/g FW, respectively. Anatomical analysis revealed no tissue damage in the epidermis, cortex and vascular bundles of the treated tomato stem. Toxicity analyses revealed that renal function parameters (blood urea and serum creatinine) and hepatic function markers (ALT and AST) were slightly altered among animals treated with CEONE at 200 µL/kg body weight. The hematological, biochemical, and histopathological analyses did not demonstrate any remarkable toxicity of CEONE on rats organs, indicating no harmful properties of CEONE. Further experimental and field trials may be advised.

Keywords: clove oil, *Fusarium oxysporum*, histopathology, nanoemulsions, tomato, toxicity, wilt.

INTRODUCTION

Tomato (*Solanum lycopersicum* L.) is one of the most cultivated worldwide and popular species of the nightshade family, Solanaceae (Padmanabhan *et al.*, 2016; Kumar *et al.*, 2024). Tomato is the most widely cultivated and consumed vegetable all over the world and is cultivated essentially in all

countries either in open fields or under protected cultivation (Lafuente *et al.*, 2023). Fusarium wilt caused by *Fusarium oxysporum* f. sp. *lycopersici* (*FOL*) is recognized globally as one of the greatest crucial diseases affecting tomatoes in both greenhouse and field and leading to significant crop losses (Maurya *et al.*, 2019; Hassan, 2020). *Fusarium oxysporum* f. sp. *lycopersici* (*FOL*) is ubiquitous, soil-borne vascular fungal

Almajed, A.A., A.M. Ismail, E.S. Elshewy, N.A.E.S. Muhanna, A.F. Hamouda and E.Y. Khafagi. 2024. Antifungal Activity of Clove Essential Oil-Based Nanoemulsion against Tomato Fusarium Wilt and Potential Toxicity on Male Albino Rats. Journal of Global Innovations in Agricultural Sciences 12:1019-1035.

[Received 20 Aug 2024; Accepted 24 Sep 2024; Published 17 Nov 2024]



Attribution 4.0 International (CC BY 4.0)

pathogen, surviving by producing two kinds of conidia, i.e., micro and macro and chlamydospores during their challenging conditions. It is particularly difficult to eradicate the disease because it creates structures known as chlamydospores, which can remain dormant in soil for a decade (Srinivas *et al.*, 2019). *FOL* comprises three races with variable virulence (Enespa, 2014), and might result in a loss of up to 10–80% of the tomato crop overall, endangering small-scale growers (Ma *et al.*, 2023). The pathogen is controlled through the use of solarization of the soil as well as the application of chemical fungicides such as methyl bromide, benomyl, or carbendazim. Managing wilt disease has been widely relied on using chemical fungicides (Amini and Sidovich, 2010). Chemical fungicides harm humans, animals, the environment, and biodiversity, according to Bawa (2016) and de Lamo and Takken (2020). Reducing losses with resistance cultivars or hybrids and fungicides (Maurya *et al.*, 2019). Even resistant cultivars to *FOL* races 1 and 2 or all three show withering symptoms, raising issues about the resistance (Oliveira *et al.*, 2023). Because of these features, fungicide use for fungal disease control must be minimized. Biocontrol is safe, cheap, and effective. It improves plant development and disease control (Castillo-Sanmiguel *et al.*, 2022). Sharifi-Rad *et al.* (2017) say essential oils (EOs) are safe, easy to extract, eco-friendly, biodegradable, and mammalian-safe. EOs consist of hydrophobic volatile aromatic compounds such as monoterpenes, sesquiterpenes, and their derivatives (Božović *et al.*, 2017; Nazzaro *et al.*, 2017; Dosoky and Setzer, 2018). Some EOs can efficiently reduce fungal development, mimicking fungicides (Palfi *et al.*, 2019; Krzyško-Lupicka *et al.*, 2020). Terpenes/terpenoids may explain EOs' antifungal activities. These chemicals fracture cell walls, kill cells, and limit fungal sporulation and germination due to their lipophilicity and low molecular weight. Many recent in vitro studies have examined EOs' Fusarium-fighting properties. Rosemary and grain mint EOs inhibit Fusarium fungus (Kumar *et al.*, 2016), clove EO (*Syzygium aromaticum* L. Merr. and L.M. Perry), and *F. Sarkhosh et al.* (2018) identified peppermint, savory, thyme, cinnamon, real lavender, eucalyptus, myrtle, and tea tree. In aqueous soil systems with disseminated pathogens, EOs' antifungal activities are severely diminished by low water solubility, high volatility, and degradation. These limits can be circumvented with oil-in-water nanoemulsion. Nanoemulsions offer advantages such as small size (<100 nm), low polydispersity, progressive bioactive component release, and reduced surfactant usage. Thus, nanoemulsions are easy-to-use colloidal delivery solutions for volatile oils in agriculture, food, cosmetics, and pharmaceuticals. Nano emulsion clove essential oil CEONE was tested in vitro and in vivo for its antifungal effects on *Fusarium oxysporum* f. sp. *lycopersici*-induced tomato vascular wilt. They also studied their indirect effects on tomato plant oxidative

enzymes (peroxidase, polyphenol oxidase), phenolic substances, carotenoids, chlorophyll, and histological changes. Following oral treatment, CEONE was tested for its anti-proliferative effects on organ function and histology in adult male rats.

MATERIALS AND METHODS

Isolation and identification of *Fusarium* fungi: Naturally infected tomato plants showing wilt symptoms were collected from different locations in Giza, Qalyubia, Sharqia, Ismailia and Beheira Governorates. Isolation was made from diseased stem and roots of wilted plants under sterilized conditions after washing in running tap water, surface disinfected with 1% sodium hypochlorite solution for two minutes, washed three times with sterilized water and dried between sterilized filter papers. The disinfected stem and roots were cut into pieces and then placed into PDA medium, and incubated at $25 \pm 2^\circ\text{C}$ for seven days. Developed fungal colonies exhibiting the taxonomic features of *F. oxysporum* (FO) were subcultured and identified according to Nelson *et al.* (1983). Further characterization of the isolated FO was done based on the amplification and sequencing of the internal transcribed spacer (ITS) region. Total genomic DNA was extracted from five FO isolates using the Dellaporta protocol (Dellaporta *et al.*, 1983). The internal transcribed spacer region (ITS) of rRNA was sequenced and amplified using primer pairs ITS4 and ITS5 (White *et al.*, 1990). The PCR process and amplification settings were as stated by Nirmaladevi *et al.* (2016) using a 2720 Thermal Cycler (Applied Biosystems, Foster City, California). The Seoul-based Macro-gene Inc. Sequencing Service cleaned and sequenced the PCR results in both directions. The NCBI GenBank database was used to assign taxonomy using the BLASTn method to compare queries to type specimens.

Pathogenicity tests

Inoculum preparation: Inoculum of the tested *FOL* isolate was prepared following the method of Sallam *et al.* (2019) by growing *FOL* on Barley grain medium. The medium was 100 g barley and 80 ml water in glass bottles. Then, the medium was autoclaved twice at 121°C for 20 min. The bottles were then, inoculated with mycelial discs of *FOL*, and incubated at $25 \pm 2^\circ\text{C}$ for 2 weeks (until medium in all bottles were covered by *FOL* mycelium)

Experimental layout: The isolated *FOL* were tested for their pathogenicity under greenhouse conditions at the Vegetable Diseases Research Department, in PPRI, (ARC), Giza, Egypt. Sterilized pots (30 cm-diameter) were filled with 3 kg of soil mixture containing sand, vermiculite, and peatmoss (1:1:2 v:v). A 2% w/w *FOL* infestation was retained in the soil for 7 days with irrigation. Twenty-five-day old healthy seedlings of tomato (super strain B) cultivar were planted in pots after 7 days of inoculation at the rate of 3 seedlings/pot. The greenhouse where day and night temperatures varied between



25–30 °C. Seedlings were watered and fertilized when necessary. The trial was carried out in a completely randomized block design with three replicates for each isolate and each replicate contained three pots. Disease severity was assessed from 2 months of planting. Control tomato seedlings were planted in uninfected soil. Fungi were re-isolated from infested tomato plants and the recovered fungi were compared with the original fungal cultures used.

Disease assessment: Two months post transplanting, of tomato plants were investigated for tomato wilt (yellowing, wilting, and vascular discoloration in the stem without any root or stem rot) disease incidence and severity. The wilt disease severity (WDS) was scored using the scale of [Waudo et al. \(1995\)](#). The DS rated using a scale of 0–5 where, 0 = no symptoms, 1 = more than (1 to 25%, 2 = more than 26 to 49%, 3 = more than 50 to 74%, 4 = more than 75 to 100%, 5 = dead plant). The wilt disease incidence % (WDI%) and wilt disease severity % (WDS%) were determined and calculated using the following formula of [Song et al. \(2004\)](#):

Disease severity %

WDS % = Σ (Number of plants \times degree of symptom) / Total number of plants \times 5 and multiplied by 100.

Disease incidence %

WDI % = Control –Treatment / Control \times 100

Preparation of CEONE: An existing technology was adapted to generate clove oil-in-water (O/W) nanoemulsion ([Mishra and Tyagi, 2018](#); [Heydari et al., 2020](#)). Clove oil was emulsified 1:2 in water using non-ionic surfactant tween 80. CEO was dropped into the aqueous phase on a magnetic stirrer at room temperature to make a coarse emulsion. For 15 minutes, a Daihan homogenizer (20,000 rpm, Korea) homogenized coarse emulsion into microemulsion and reduced oil droplet size. Stage one for CEONE.

Formulation of CEONE: The pre-formulated microemulsion was sonicated using a probe sonicator (Model LC 60/H, Elma, Germany) using a 12 mm diameter sonication probe. The sonication process was carried out at a frequency of 20 kHz and a power of 400 W. For stability reasons, the CEONE was placed in an ice bath during the sonication process to prevent overheating. Sonication was performed for a total of 15 minutes, with a duration of 10 seconds of sonication followed by 5 seconds of rest ([Salvia-Trujillo et al., 2013](#)). Finally, the prepared CEONE was kept under cool at 4 °C for further work.

Characterization of CEONE: The size and surface charge nanodroplets of the prepared CEONE was detected through dynamic light scattering (DLS) technique using Malvern Zeta Sizer instrument, UK. To decrease the viscosity of the CEONE and minimize the multiple scattering effects during the measurements, the CEONE was diluted with deionized water. DLS analyses the Brownian motion of the nano-sized droplets in the CEONE providing information about their hydrodynamic diameter in nanometer (nm). Furthermore, the zeta potential was determined to estimate the surface charge

of the nanodroplets and consequently their electrophoretic mobility.

Morphological examination: CEONE was diluted with deionized water and examined under a transmission electron microscope (TEM, Jeol, USA) to determine its shape and size. After phosphotungstic acid staining, a tiny droplet was examined on a copper grid.

Antifungal activity of CEONE and CEO against *FOL*

Laboratory trials: The fungistatic activity of CEONE and CEO were evaluated against *FOL* on PDA medium using food poisoning method as described by [Afifi et al. \(2017\)](#). CEONE was used at concentrations of 50, 100, and 200 µL/L, while CEO was used at concentrations of 500, 1000 and 1500 µL/L. Treatments were added to determined amounts (100 ml) of PDA medium and mixed well for the homogeneity. After reasonable cooling to 45 °C, aliquots of 15 mL of the PDA medium were poured into Petri dishes with a diameter of 90 mm. Fungal cultures growing on PDA medium without CEONE or CEO were served as controls. Uniform fungicide was used as a control. Discs of 5-mm mycelial growth of *FOL* was taken from 7-days-old culture and plated out in the centrally placed of each Petri dish and incubated at 25 ± 2 °C. Four replicates with three plates for each treatment. The plates were daily observed until fungal growth covered the surface of the medium in any treatment. After incubation, colony diameter (mm) of each plate was measured by averaging the two diameters taken at right angles for each colony. Percentage of radial growth decrease in each treatment was calculated using [Sirirat et al. \(2009\)](#) formula:

$$\text{Reduction \%} = \left(\frac{d_e - d_i}{d_e} \right) \times 100$$

Where, d_e = is diameter of radial growth in the control, d_i = mean diameter of radial growth in the treatment.

Greenhouse trials

Pot experiments: Inoculum preparation and inoculation were followed as previously mentioned under pathogenicity tests. Tomato seedling were dipped in different CEONE concentrations 50, 100 and 200, and CEO at 500, 1000 and 1500 µL/L. Likewise, the fungicide Uniform® was applied at dose of 1 mL/L by soaking tomato seedlings for 30 minutes prior planting. As mentioned in the pathogenicity test section, [Song et al. \(2004\)](#)'s formula was used to calculate WDI% and WDS%.

Biochemical analyses: Biochemical properties of transplanted tomato plants were examined after 40 days. [Ismail and Abd El-Gawad \(2021\)](#) filtered crude extract from 1 g leaves in 50 mL of phosphate buffer solution (7.1 pH) through five cheesecloth layers. The filtrate was centrifuged at 3000× g for 15 minutes. Activity was tested with clear supernatants as crude enzymes. The APEL Co., Ltd. Japan PD-303 spectrophotometer measured enzymes calorimetrically every 10 s for 1 min. Change in absorbance per minute per gram fresh weight (g FW) was measured three times.



Determination of chlorophyll and carotenoid: The amount of chlorophyll a and b were calorimetrically measured at wavelengths 645 nm and 663 nm, respectively using the method of Arnon (1949), and the following equations:

$$\text{Chlorophyll a (mg/g FW)} = 12.7 (\text{A663}) - 2.69 (\text{A645})$$

$$\text{Chlorophyll b (mg/g FW)} = 22.9 (\text{A645}) - 4.68 (\text{A663})$$

$$\text{Total chlorophyll (mg/g FW)} = 20.2 (\text{A645}) + 8.02 (\text{A663})$$

Where, A = Absorbance at respective wavelength = FW = Fresh weight of the sample (g).

The amount of carotenoid was calorimetrically determined at wavelength 480 nm following the method of Kirk and Allen (1965) using the following equation:

$$\text{Carotenoids (mg/g FW)} = \text{A480} + (0.114 \times \text{A663}) - (0.638 \times \text{A 645})$$

Where, A = Absorbance at respective wavelength.

Determination of total phenolic content: Total phenolic content was calorimetrically measured at wavelength 540 nm following the method described by Snell and Snell (1953) and was presented as mg phenolics per gram of fresh weight.

Determination of enzyme activity

Peroxidase assay (PO): The Kar and Mishra (1976) approach was used to assess peroxidase activity. After adding one milliliter of crude enzyme extract to five milliliters of the solution (1.5 mL of phosphate buffer pH 6.8, 3 ml of 0.05 M pyrogallol), the reaction was halted with 0.5 mL of 1% H₂O₂. The color intensity was calorimetrically measured at 420 nm after five minutes at 25 °C.

Polyphenol oxidase assay (PPO): Kar and Mishra (1976) calculated polyphenol oxidase (PPO). Five milliliters of the solution (3.5 ml phosphate buffer pH 6.8, 3 ml 0.05 M pyrogallol) were mixed with one milliliter of crude enzyme extract. Color intensity was calorimetrically evaluated at 420 nm by spectrophotometer after 5 min at 25 °C.

Histopathological examinations: For histological studies, Anjum *et al.* (2016) immersed 10 mm transverse sections of collar roots of healthy and diseased tomato plants in formalin acetic acid (5%, v/v formalin 10%, distilled water 35%, and ethyl alcohol 50%) for the fixed samples were kept in 75% ethanol, 25% acetic acid. Under a light microscope, samples examined.

Field experiment: The experiments were carried out under naturally infected fields at Sharqia and Qalyubia governorates. The treatments were designed as described in the section of greenhouse experiments. A complete randomized block design with three replicates for each treatment, irrigation, fertilization was carried out as recommended. The disease symptoms were observed at 60 days post-inoculation. The wilt disease incidence % (WDI%) and wilt disease severity % (WDS%) were determined and calculated as described under pathogenicity test title.

Anti-proliferative effect of CEONE on rats

Experimental design: The 21 male albino rats, weighing 150–160 grams, were placed into three groups of seven. At the Faculty of Veterinary Medicine, Benha University, rats

from the National Research Center in Egypt were kept at 21–22°C with a 12-hour light/dark cycle. Participants received water and normal food pellets for 20 days. Rats acclimated to laboratory conditions over a one-week period. Experimental protocols adhered to ethical standards (BUFVTM 03-01-23). The rats were divided into three groups: group 1 (negative control) received 1 ml of maize oil daily for 20 days, group 2 received 0.5 ml/kg body weight of CCL4 (positive control), and group 3 received 200 µl of CEONE daily. Blood samples were collected via cardiac puncture into vacutainers containing and lacking EDTA for durations of 10 and 20 days during the trial.

Body and organ weights: Rats in all the groups were weighed the first and the last day of study Seth *et al.* (1972). The body weight (bw) gain (g) was calculated using the following equation: Body weight gain (g) = final bw – initial bw. The relative liver weight was calculated using the final bw and absolute liver, kidney, spleen and heart weight according to the following equation:

$$\text{Relative organ weight \%} = (\text{Absolute organ weight (g)} / \text{Final body weight (g)}) \times 100.$$

Hematological analysis: Whole blood Hb, PCV%, and erythrocyte count were measured. Electronic cell counters (VetScan HM5 Hematology system, Abaxis, Inc., Union City, CA, USA) measured total and differential leukocyte counts.

Serum biochemical analysis: Sera collected from blood were analyzed to quantify the alanine transaminase (ALT) and aspartate transaminase (AST) (Bergmeyer *et al.*, 1977), and the concentration of Urea and creatinine (Patton and Crouch, 1977; Jaffé, 1986). Total Antioxidant Capacity (TAC)) (Erel, 2004), Malondialdehyde (MDA) (Ruiz-Larrea *et al.*, 1994), Nitric Oxide (NO) (Montgomery and Dymock, 1961) and TNF- α (Aydin, 2015) were assessed.

Histopathological examination: Each group's butchered liver, kidney, and spleen tissues were fixed in 10% neutral buffered formalin for 24 h. Following dehydration and cleaning, tissues were imbedded in paraffin wax. Histopathological examinations were performed on five H&E-stained µm sections. All histology procedures were conventional (Bancroft, 2002).

Statistical analysis: The obtained data were subjected to analysis of variance one-way ANOVA using the CoStat program. The treatment means were compared by the Least Significant Differences (LSD) at the 5% probability level were assessed according to Gomez and Gomez (1984).

RESULTS AND DISCUSSION

Molecular characterization of FOL: FOL was isolated from diseased tomato plants for molecular determinations. Polymerase chain reaction (PCR) amplicons of approximately 350 bp to 500 bp were obtained for ITS gene region. BLAST analysis of the ITS rDNA sequence data validated morphological identification, with *Fusarium oxysporum* f. sp.



lycoperisici being the closest 100% similarity in NCBI GenBank. The NCBI GenBank database contains the seven strains' ITS rDNA sequences (PP992518–PP992524). Management of wilt diseases requires precise pathogen identification and genetic characterization. In our study, ITS region revealed as satisfactory identification of *FOL* isolates. Previous studies confirmed our findings and demonstrated that ITS region has been widely used and effective to identify *Fusarium* at species level (Singha *et al.*, 2016; Isaac *et al.*, 2018; Sallam *et al.*, 2019).

Pathogenicity tests of *FOL*: Figure (1) showed that the seven isolates of *FOL* representing the seven districts were considerably different regarding aggressiveness against (Super Strain B) tomato plants. The isolate FOL-EG3-2022 derived from Sharqia significantly exhibited the highest wilt disease incidence (WDI%) and wilt disease severity (WDS%) being (96.29% and 40.29%) respectively, followed by Qalyubia isolate FOL-EG4-2022 (70.37% and 32.59%), Ismailia isolate FOL-EG1-2022 (55.56 and 21.16%) and Beheira isolate FOL-EG2-2022 (44.44 and 18.42%). On the other hand, both Giza isolates FOL-EG5-2022 and FOL-EG6-2022 showed the lowest WDI% and WDS% with values recorded (25.92 and 26.28%) and (29.63 and 15.39%). Variation in aggressiveness of *FOL* isolates on tomato plants may be due to the presence of genetic variation among the isolates. These differences in aggressiveness were also pointed by other authors (Joshi *et al.*, 2013; Isaac *et al.*, 2018; Abdulkadir *et al.*, 2023). Furthermore, Steinkellner *et al.*, (2005) reported that the pathogenicity of *FOL* in tomato could be affected by the race, internal factors such as enzymes, growth-regulating compounds, toxins, environmental and growing conditions. In the present study, the control tomato plants remained healthy or symptomless. *FOL* infestation was further recovered from the wilted plants and the identity was compared with original isolate.

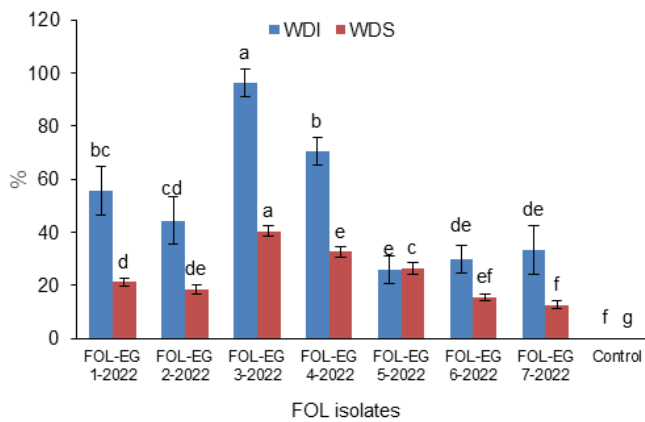


Figure 1. Pathogenicity test of seven isolates of *FOL* representing five different locations of isolation. The values expressed within columns represent the average of three repetitions \pm standard deviation. According to the LSD

test, bars denoted by distinct letters varied significantly ($p < 0.05$).

Characterization of CEONE: Zeta size distribution showed that the procedure produced CEONE with nanodroplets 50.75 nm ideal size, ensuring good stability (Figure 2A). Moderate polydispersity (0.854) value shows stable and homogeneous NE nanodroplets with uniform size distribution. Zeta potential showed CEONE surface charged droplets exceeding -37.6 mV (Figure 2B). Some investigations found that nanoemulsions with surface charges greater than +20 mV or -20 mV are highly stable due to strong repulsive forces among their oily droplets (Heurtaul *et al.*, 2003). According to previous studies, strong electrostatic forces that maintain particles' stability and dispersion are indicated by high zeta potential levels (Pochapski *et al.*, 2021). Extremely positive or negative zeta potential values exert greater repulsive forces, while repulsion between particles with equivalent electric charges inhibits aggregation and allows simple redispersion and stability (Honary and Zahir, 2013; Ali *et al.*, 2016). For single layer nanoemulsion (SLN) stability, tween 80 provides steric stability (Hoeller *et al.*, 2009).

The TEM images revealed that CEONE had uniform spherical nanodroplets (Figure 2C), similar to documented previous literature reporting the successful formation of nanoemulsions with spherical oily nanodroplets (Anjali *et al.*, 2012; Ghosh *et al.*, 2013). The size noticed from TEM images (Figure 2C), however, were slightly smaller than those obtained from zeta sizer measurements (Figure 2A). This is attributed to the hydrodynamic effect of abundance of nanoformulations suspended in water compared to the dried samples investigated through TEM analysis (Delan *et al.*, 2022; Ali *et al.*, 2023).



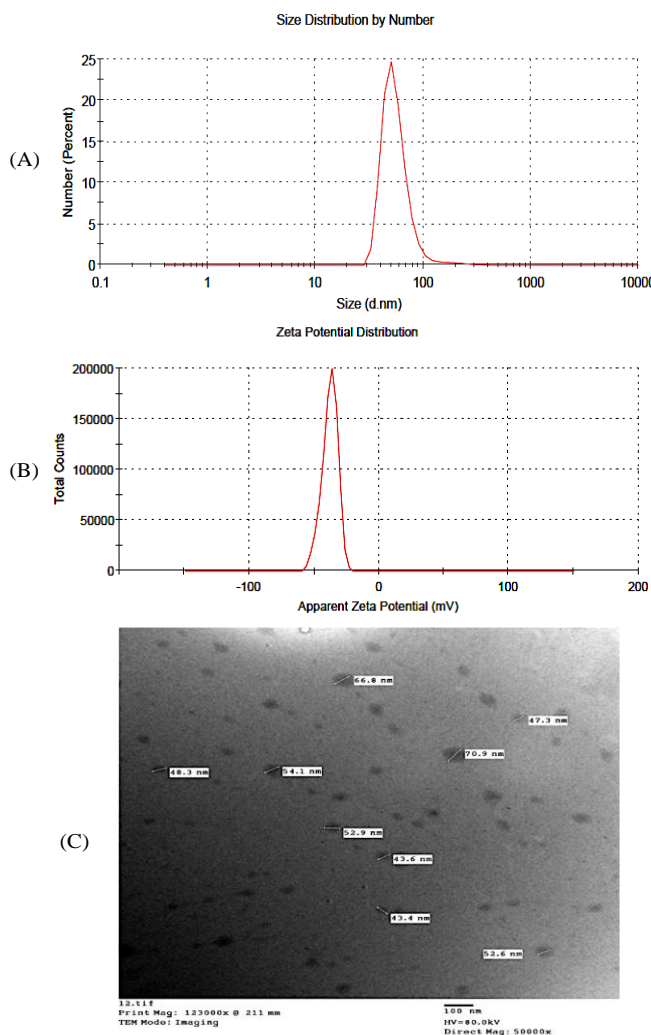


Figure 2. Zeta size (A), potential distribution (B) and TEM imaging of prepared CEONE (C).

Antifungal activity of CEONE and CEO against FOL: Data in Figure 3 indicate that the tested CEONE, CEO and Uniform fungicide have affected significantly ($p < 0.05$) the growth of *FOL*. CONE at concentration of 200 μ L/L showed the highest inhibition calculated as at 78.06% and the percentages have dropped to 64.17%, and 44.72% at 100 μ L/L and 50 μ L/L, respectively. On the other hand, Uniform fungicide exhibited significantly ($p < 0.05$) the highest decrease in the mycelial growth up to 1.22 mm with an inhibition percentage reached 85.56 %. Meanwhile, CEO displayed the lowest inhibition against mycelial growth at concentrations of 500, 1000, and 1500 μ L/L (26.39, 38.89 and 52.22%), respectively. CEO and CEONE exhibit differing antifungal activity due to their hydrophilic or lipophilic primary components (Ghabraie *et al.*, 2016). CEONE functioned better than CEO and FOL, even at low doses (50 μ L/L). Nanoemulsions are better than regular ones due to their small size, large surface area,

progressive active ingredient release, and stability, according to Muhtaq *et al.* (2023). In Attia *et al.* (2023), thyme oil nanoemulsion (TONE) at doses 1, 2, 3, and 4 mg/ml decreased *F. oxysporum* growth by 7.78, 31.1, 52.2, and 67.8% Eugenol, a major component of CEO, is more water-soluble in CEONE than CEO, which may explain its maximal inhibitory activity. According to He *et al.* (2016), micro-emulsifying clove oil boosted its *Penicillium digitatum*-antifungal potential. CEO in nano emulsion may be more effective against fungi because the smaller droplet size increases oil content in the cell, distorting the phospholipid bilayer (Tao *et al.*, 2014).

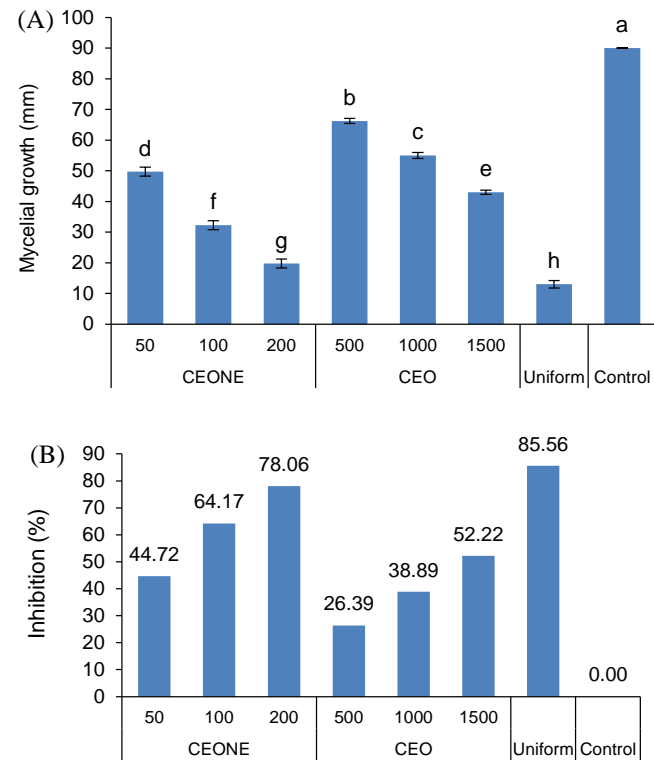


Figure 3. Antifungal effect of CEONE, CEO and uniform fungicide against the mycelial growth (A) and inhibition % (B) of *FOL*. The values within columns represent the average of three replicates \pm standard deviation. The LSD, bars denoted by distinct letters varied significantly ($p < 0.05$).

Greenhouse trial: Table 1 shows that the symptoms of Fusarium wilt were very clear and WDI reached the maximum rate by 100% in infected tomato with Fusarium treatment only. Application of CEONE at high concentration of 200 μ L/L decreased the WDI to 14.81% and WDS to 5.19%, with an efficacy reached 85.19 and 87.72 %, respectively. Our findings are supported by those previously published, of which tomato Fusarium wilt incidence has been efficiently reduced by treating soil mixtures with aqueous emulsion of clove oil (Sharma *et al.*, 2018). Similarly, the study of Attia



Table 2. Effect of CEONE, CEO and Uniform fungicide on WDI and WDS of tomato Fusarium wilt under field conditions.

Treatments	Conc. (µL/L)	Sharqia				Qalyubia			
		WDI %	Efficacy %	WDS %	Efficacy %	WDI %	Efficacy %	WDS %	Efficacy %
CEONE	50	44.44 ^b	25.93	23.96 ^{bc}	27.70	26.67 ^{ab}	29.42	20.17 ^b	25.58
	100	31.11 ^{bc}	48.15	21.48 ^c	35.18	24.44 ^{bc}	35.30	16.41 ^{cd}	39.43
	200	20.00 ^{cd}	66.67	12.95 ^e	60.92	13.33 ^{cd}	64.71	11.15 ^e	58.84
CEO	500	44.44 ^b	25.93	26.05 ^b	21.40	28.89 ^{ab}	23.54	22.91 ^b	15.45
	1000	33.33 ^{bc}	44.45	23.31 ^{bc}	29.67	26.67 ^{ab}	29.42	19.70 ^{bc}	27.29
	1500	26.67 ^{cd}	55.56	16.90 ^d	49.01	20.00 ^{bcd}	47.06	15.63 ^d	42.32
Uniform (1mL/L)		13.33 ^d	77.78	8.01 ^f	75.84	8.89 ^d	76.47	7.04 ^f	74.01
Control Infected		60.00 ^a	0.00	33.14 ^a	0.00	37.78 ^a	0.00	27.10 ^a	0.00
LSD at 5 %		15.049		3.839		12.041		3.527	

Values expressed within columns represent the average of three replicates and means marked with different letters denote significant differences (LSD, $p < 0.05$).

et al. (2023), revealed that thyme oil nanoemulsion (TONE) reduced DI of Fusarium tomato wilt up to 42.5% with protection percentage 50%. Additionally, *Aravena et al.* (2021), found out that nanoemulsion based on *Psoralea* plant extract reduced the advance of *FOL* when applied at 500 ppm. In this study, the Uniform fungicide exhibited significantly the highest decrease in WDI and WDS by approximately two-fold than CONE and recorded 7.41 and 4.45%, respectively. Moreover, the efficacy of Uniform fungicide has reached up to 92.59% for WDI and 89.47% for WDS respectively; however, it also entails a higher cost per hectare and increased hazards of damage to the environment and the applicator. By contrast, CEO displayed unsatisfactory decrease in WDI and WDS when applied at low concentration, however, the high concentration of CEO (1500 µL/L) exhibited equal effect to the concentration (100 µL/L) of CEONE with values of recorded 25.92% and 11.11% WDI and WDS. Similar research study demonstrated that CEO had a MIC and minimum bactericidal concentrations (MBC) only when applied at high concentrations as 400 and 500 µL L⁻¹, respectively against *Pectobacterium carotovorum* subsp. *carotovorum* (*Zhang et al.*, 2023). Hence these published findings along with ours, revealed that CEO in bulk form poses antifungal activity only when applied at high concentrations.

Table 1. Effect of CEONE, CEO and Uniform fungicide on WDI and WDS values of tomato Fusarium wilt under greenhouse condition.

Treatments	Con. (µL/L)	WDI %	Efficacy %	WDS %	Efficacy %
CEONE	50	37.03	62.97	14.07	66.67
	100	25.92	74.08	11.11	73.69
	200	14.81	85.19	5.19	87.72
CEO	500	40.74	59.26	17.78	57.90
	1000	37.03	62.97	17.01	59.72
	1500	25.92	74.08	11.11	73.69

Uniform (1mL/L)	7.41	92.59	4.45	89.47
Control Infected	100.0	0.00	42.22	0.00
Control Healthy	0	100.0	0.00	100.0
LSD at 5 %		9.615		4.129

Values expressed within columns represent the average of three replicates and means marked with different letters denote significant differences (LSD test, $p < 0.05$).

Field trial: Data in Table 2 shows that the treatment of CEONE and CEO have decreased the WDI% and WDS% in comparison with the control with differences among them. The WDS and WDS revealed significant variances ($p < 0.05$) among the treatments in both locations. In this respect, treatment with 200 µL/L CEONE displayed great efficacy in decreasing WDI (66.67 and 60.92 %) and WDS (64.71 and 58.84%) in both Sharqia and Qalyubia experiments, respectively. However, the control treatment, it remained it was significantly ($p < 0.05$) effective. Similar to our findings, *Sharma et al.* (2018), reported that nanoemulsion containing clove (CO) and lemongrass oil (LGO) applied as a soil amendment has decreased the WDS up to 70.6% compared with untreated control. Furthermore, an earlier study demonstrated that eugenol oil nanoemulsion showed fungicidal activity against *F. oxysporum* f. sp. *vasinfectum* the causative agent of wilt disease of cotton (*Abd-Elsalam and Khokhlov*, 2015). Obviously, the treatment with the Uniform fungicide significantly had the greatest inhibitory effect, recording low WDI (13.33 and 8.89) and WDS (8.01 and 7.04) in both Sharqia and Qalyubia experiments, respectively. Nevertheless, the highest WDI and WDS values were observed for plants treated with the CEONE (50 µL/L) and CEO (500 µL/L), indicating that they had the lowest efficacy in decreasing WDI and WDS of *FOL*. One of the major apprehensions of using bulk essential oil-based formulation as soil amendments is the requirement of higher doses to control soil-borne pathogens (*Sharma et al.*, 2018). This coincided with our finding, of which the inhibitory effect of CEO showed dose-dependent activity against *FOL* wilt



disease. Thus, these findings along with ours, revealed that essential oils at bulk poses antifungal activity only when applied at high concentrations.

Antioxidant enzymes activity: Tomato plants treated with CEONE, CEO, and Uniform fungicide exhibited significantly higher peroxidase (PO) and polyphenol oxidase (PPO) activity ($p < 0.05$) compared to untreated or healthy plants (Figure 4). Compared to CEONE and CEO at all concentrations, uniform treatment at 1m/L dose considerably ($p < 0.05$) enhanced PPO and PO levels in tomato plants. [Ismail and Abd El-Gawad \(2021\)](#) found that penconazole fungicide treatment increased pepper plant PO activity more than MgONPs and ZnONPs. However, CEONE and CEO at 100 and 1000 $\mu\text{L}/\text{L}$ concentrations considerably ($p < 0.05$) increased PPO levels. In contrast, high concentrations of CEONE and CEO substantially ($p < 0.05$) reduced PPO levels. CEONE and CEO treatments had varying effects on PO activity.

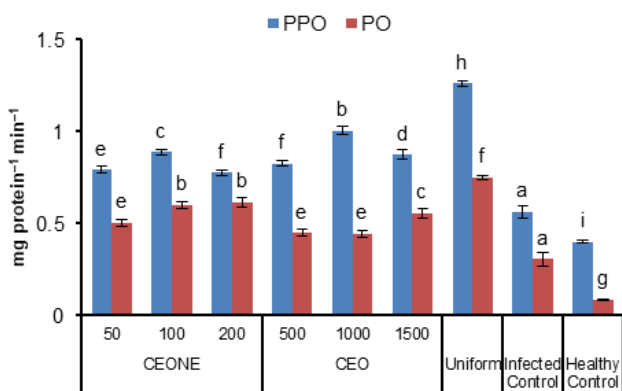
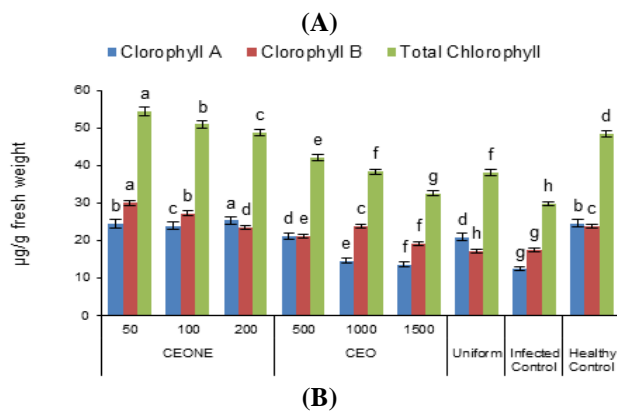


Figure 4. Peroxidase activity (PO) and polyphenol oxidase activity (PPO) in infected tomato plants treated with CEONE, CEO and Uniform fungicide. The values expressed within columns represent the average of three replicates \pm standard deviation. According to the LSD test, bars denoted by distinct letters varied significantly ($p < 0.05$).

Furthermore, no significant difference was observed in PO level in tomato plants treated with CEONE at concentrations 100 and 200 $\mu\text{L}/\text{L}$. Notably, a slight increase in the PPO and PO activity was noted in untreated infected plants. This increase might be attributed to the response of the infected plant defense system for limiting the disease spread ([Kaur et al., 2022](#)). The PO and PPO enzymes plays a vital role in cellular defense against oxidative stress induced by plant pathogens and one of the key control mechanisms for cellular protection against various diseases ([Ismail and Afifi, 2019; Ismail, 2021; Zulfiqar and Ashraf, 2022; Almaghasla et al., 2023](#)).

Total chlorophyll, phenols and carotenoid content: Determination of chlorophyll content can serve as an indicator of plant health and photosynthetic activity ([El-Beltagi et al., 2024](#)). In this regard, all treatments resulted in

a significant ($p < 0.05$) increase in chlorophyll content (a, b, or total chlorophyll) compared with control plants (Figure 5A). Out of all treatments, CEONE was superior in increasing total chlorophyll at concentrations of 50, 100 and 200 $\mu\text{L}/\text{L}$, with values 48.69, 50.90 and 54.41 $\mu\text{g}/\text{g FW}$, respectively. The greatest decrease in chlorophyll content was recorded in untreated infected control plants. This decrease in total chlorophyll plants as may be a consequence of the fungus *FOL* effect on the release of leading to inhibition the chlorophyll biosynthesis ([Achore et al., 1993](#)). In the present work, the high concentrations of CEONE and CEO caused significant ($p < 0.05$) decrease in chlorophyll content (a, b, or total chlorophyll). Carotenoids content in tomato plants decreased significantly ($p < 0.05$) with high CEONE concentrations. Also, the treatment with CEO at all concentrations resulted in a marked increase in the carotenoids content with no significant differences among them. Chlorophyll a and carotenoids are linked. Plants interpret increases in this pigment as a signal to enhance carotenoid biosynthesis ([Bartucca et al., 2020](#)). Based on our findings and [Mosa et al. \(2023\)](#), nanoemulsions should be used in moderation to reduce illnesses and promote the synthesis of good substances. In tomato plants, CEONE at 200 $\mu\text{L}/\text{L}$ and CEO at 1500 $\mu\text{L}/\text{L}$ significantly increased phenol content compared to other treatments and healthy plants (Figure 5C). CEO, a potent antioxidant rich in phenolic acids, may explain this increase ([Brewer, 2011; Hashem et al., 2023](#)). Along with developing cell walls, antioxidants capture free radicals and protect plant cells ([Sharma et al., 2018](#)).



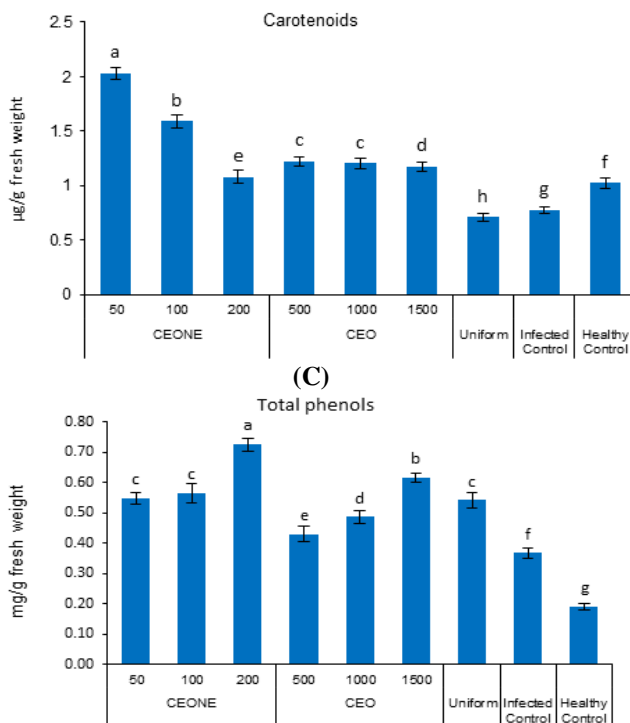


Figure 5. The level of chlorophyll (A), carotenoids (B) and phenols content (C) in tomato plants in response to treatments with CEONE, CEO and Uniform fungicide in relative to infected and healthy controls. The values expressed within columns represent the average of three repetitions \pm standard deviation. According to the LSD test, bars denoted by distinct letters varied significantly ($p < 0.05$).

Histological studies of plants: The anatomical observations (Figures 5) of stems of treated tomato plants revealed positive changes in the water conductive elements particularly xylem and width of the vascular bundles in CEONE and CEO treated tomato plants, (Figure 6A, B and C). The root-stem transition zone demonstrated that FOL mycelia entered plant tissue less in CEONE and CEO-treated plants (Figure 6A, B, and C) than in untreated control plants (Figure 6D and E). However, tylosis formation and changes in collenchyma cell, phloem, cambium and cortical parenchyma may also be attributed to hypertrophy in response to infection. A similar finding is reported by [Rahman et al. \(1999\)](#), who stated that tylosis formation is a common defense response in xylem vessels against vascular wilt pathogens such as *Fusarium oxysporum*, *Verticillium albo-atrum* and *R. solanacearum*. Tylosis formation and *Fusarium* hyphae were clearly seen in the tissue treated with CEO (Figure 6B). Figure 6D shows fungal structures and xylem fiber destruction relative to healthy tissues, as well as plant defensive tylosis synthesis. Hyperplasia and hypertrophy may also trigger pathogen invasion and phloem cell death ([Beckman, 1987](#); [Beckman](#)

and [Roberts, 1995](#)). Healthy tissues have three collenchyma and two parenchyma layers in their cortex (Figure 6E). Essential oils have been shown to directly affect fungal mycelia structure ([Perczak et al., 2019](#)), but their ability to reduce plant disease severity has never been shown in plant tissue anatomical investigations.

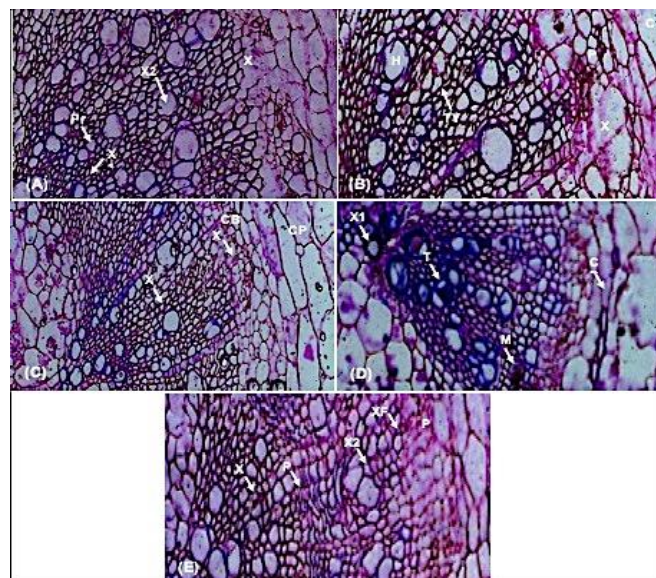


Figure 6. Cross section in the tissues of collar roots of tomato plants treated with CEONE (A); CEO (B), Uniform fungicide (C), and infected tomato without treatments (D) and uninfected tomato (E). Ep, epidermis; Co, collenchyma; Cp, cortical parenchyma; Cb, cambium; X1, primary xylem; X2, secondary xylem; Pr, ray parenchyma cells; Xf, xylem fibers; P, phloem; Pe, periderm, Co collenchyma cell; H, hyphae of *FOL*; M, microconidia of *FOL*; T, Taylosis; Ty, Tylosis formation starts.

Toxicity of CEONE on male albino rats

Body and relative organ weights: Oral CEONE delivery at 200 μ l/kg bw did not cause any deaths or adverse effects during the 20-day investigation. Daily observations over the experimental period of 20 days showed no detectable alterations in the general states of the animals in all groups. Rats administered to CCl4 at 0.5 ml/kg bw exhibited a significant ($p < 0.05$) decrease in body weight (g) after 20th day. Furthermore, there was a significant ($p < 0.05$) increase in liver and kidney weights in the CCL4-treated rats when compared to CEONE-treated rats and the untreated negative control group. No significant ($p < 0.05$) differences were noticed between CEONE-treated group and untreated negative group in terms of liver, and heart weights. However, there was significant ($p < 0.05$) differences were noticed between CEONE-treated group and the untreated negative group in body, kidney, and spleen weights, but these



Table 4. Effect of CEONE and Carbon Tetrachloride (CCL4) on hematological picture of rats.

Treatments	WBCs (x10 ³ /μl)		RBCs (x10 ⁶ /μl)		HB (mg/dl)		PCV (%)	
	10 th day	20 th day	10 th day	20 th day	10 th day	20 th day	10 th day	20 th day
CEONE	36.17a	15.47b	2.90a	3.45a	8.6a	10.0a	24.85a	28.87a
CCL4	28.5b	11.50c	3.05a	2.67b	8.95a	9.03a	25.8a	26.1a
Control	22.1c	19.66a	3.28a	3.57a	8.9a	8.53a	25.95a	24.67a

Abbreviations: WBC, white blood cells; RBC, red blood cells; Hb, haemoglobin; PCV, packed cell volume. Means within the same row followed by different letters are significantly different (p < 0.05).

differences were not high. The direct and indirect toxicity of CCl4 caused changes in body weight and liver weight in rats (Shi *et al.*, 1998). Thus, this relative liver weight change indicates acute hepatic injury (Fukao *et al.*, 2004). Interestingly, insignificant (p < 0.05) changes between CEONE-treated rats and the untreated negative group confirmed that CEONE may be recognized as safe.

Table 3. Effect of CEONE and Carbon Tetrachloride (CCL4) on body and relative organ weights of rats.

Treatment	Weight gain (g)	Liver	Kidney	Spleen	Heart
		weight %	weight (%)	weigh (%)	weight (%)
CEONE	41.30b	2.52b	0.47c	0.42a	0.31a
CCL4	26.33c	5.43a	0.64a	0.31c	0.24b
Control	66.27a	2.62b	0.49b	0.38b	0.30a

Means within the same row followed by different letters are significantly different (p < 0.05).

Hematological examinations: Hematological parameters are generally considered one of the most sensitive sets of parameters to assess the safety of any material (Bloom, 1993). Table 4 revealed a significant (p < 0.05) increase on the 10th day in WBCs in CEONE and CCL4-treated animals relative to the untreated negative control group. While, after the 20th day, CCL4-treated rats showed a significant (p < 0.05) decrease in WBCs and RBCs when compared to CEONE-treated and negative control animals. These data showed a decrease in WBCs and RBCs, likely due to a toxic effect on bone marrow and hematopoiesis (Shalaby *et al.*, 2011). No significant changes noticed in the packed cell volume % (PCV%) and hemoglobin concentration (Hb) between CEONE and CCL4 treatments animals in relative to untreated negative control group (Table 4). Our findings, indicated the safety use of CEONE, and supported with those obtained by Vijayasteltar *et al.*, (2016).

Serum biochemical parameters: CEONE-treated mice had significantly increased blood urea and serum creatinine levels (p < 0.05) compared to untreated control animals (Table 5). CEONE-treated mice had no change in ALT or AST (Table 5). A prior trial found no mortality, adverse effects, clinical or behavioral symptoms, or hematological or biochemical abnormalities with Clovinol at 2 g/kg bw (Issac *et al.*, 2015). Our findings are supported by those reported earlier by

Shalaby *et al.* (2011), who reported that clove oil did not produce any significant changes in renal function parameters (urea and serum creatinine). Due to the presence of eugenol, CO has a protective effect against lipid peroxidation and has an anti-genotoxic impact (Sharma *et al.*, 2011). However, in this study, a decreasing trend on renal function parameters and hepatic function markers have been observed among animals treated with CCl4 at 0.5 ml/kg bw. The renal alterations caused by CCl4 are possibly mediated by oxidative stress, while CEONE is enriched with many antioxidant compounds (Ogata *et al.*, 2000). Furthermore, Ahmed *et al.* (2011) and ELSayed *et al.* (2019) reported that CCl4-induced hepatotoxicity by its oxidative stress, which confirmed by increased serum liver enzymes (ALT and AST).

Table 5. Effect of CEONE and Carbon Tetrachloride (CCL4) on renal function parameters and hepatic function markers of rats.

Treatments	ALT U/L	AST U/L	Urea mg/dl	Creatinine mg/dl
CEONE	24.63b	66.26b	36.50b	0.71b
CCL4	93.13a	94.95a	60.53a	1.43a
Control	22.60c	62.14c	32.8c	0.48c

Abbreviations: ALT, alanine aminotransferase; AST, aspartate aminotransferase; ALP, alkaline phosphatase. Means within the same row followed by different letters are significantly different (p < 0.05).

Antioxidant and oxidative stress markers: Table 6 revealed a significant (p < 0.05) elevation in TAC in CEONE-treated animals. This may be due to the clove is a rich source of bioactive compounds especially phenolic compounds indicating its antioxidative effects (El-Maati *et al.*, 2021). Furthermore, the CCL4-treated animals recorded a significant (p < 0.05) increase in MAD and NO levels when compared to CEONE-treated animals and negative control. This was also reported by Ahmed *et al.*, (2011) and EL Sayed *et al.*, (2019), who reported that CCL4-treated animals, displayed high levels of NO and MAD. However, their level was higher in CEONE-treated animals when compared to CCL4-treated animals, and this could be due to eugenol as the main antioxidant compound in clove oil (Ogata *et al.*, 2000). On other hand, the present results recorded that significant elevation of TNF-α in CCL4 and CEONE treated animals when compared to the control negative group (Table 6). This



increase may be due to tissue damage associated with hepatic inflammation caused by CCL4 dosing can be mediated by the proinflammatory cytokines such as inducible TNF- α (Ma *et al.*, 2014).

Table 6. Effect of CEONE and Carbon Tetrachloride (CCL4) on the oxidative stress markers.

Treatments	TAC mmol/l	MAD mmol/l	NO nM/gm	TNF- α Pg/ml
CEONE	5.70a	42.83b	10.27b	40.56b
CCL4	0.87c	92.53a	25.2a	65.57a
Control	1.46b	25.07c	5.57c	20.66c

Abbreviations: TAC, total antioxidant capacity; MDA, malonaldehyde; NO, nitric oxide; TNF- α , Tumor Necrosis Factor- α . Means within the same row followed by different letters are significantly different ($p < 0.05$).

Histopathological analysis: The microscopic analysis of untreated rats' liver parenchyma tissues indicated no morphological alterations (Figure 7A). In contrast, CCL4-treated mice had diffused fatty alterations throughout hepatocytes in the lobules (Figure 7B). Our findings are in agreement with those previously published by Wu *et al.* (2017), with regard to the CCl4-induced hepatotoxicity by its oxidative stress and caused diffused fatty change all over the hepatocytes. Examination of liver tissues of CEONE treated animals showed that the structure of the hepatocytes appeared more or less like normal, however, fatty change in individual hepatocytes in the focal manner (black arrow) was observed indicating that CEONE is permanent non hepatotoxic but for short period (Figure 7C). Comparable results were also reported by Shalaby *et al.* (2011), who indicated that CEO did not affect the structure of the hepatocytes. In the untreated control group, the kidney cortex's glomeruli and tubules showed no histological changes (Figure 7D). CCL4-treated mice had perivascular edema and inflammatory cell infiltration around the cortex's dilated blood vessels (Figure 7E). Histopathological changes such oedema from cortical tubular lining degradation were also present. This supports earlier findings that CCl4 is hepatotoxic and nephrotoxic due to free radicals that damage DNA, proteins, and lipids (Ronis *et al.*, 1998; Natarajan *et al.*, 2006; Makni *et al.*, 2012). In addition, CEONE-treated animals' kidneys demonstrated modest degenerative alterations in tubular epithelium near the cortex (Figure 7F).

.

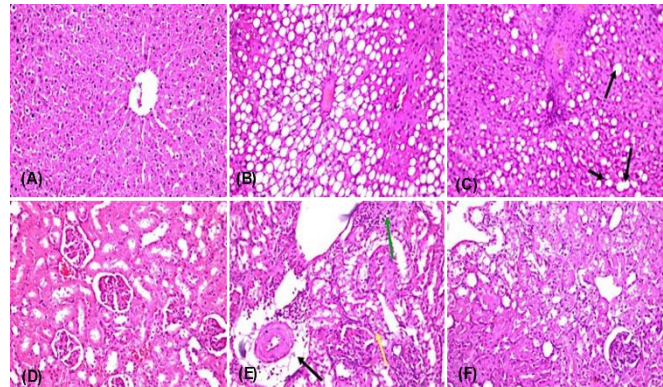


Figure 7. Histopathological features of liver, (A) untreated negative control group of rats showed normal structure of the central vein and surrounding hepatocytes in lobules of the parenchyma; **(B)** hepatocytes of liver of CCL4 treated animals showed diffuse fatty changes all over hepatocytes in the lobules of parenchyma; **(C)** histopathological features of hepatocytes of CEONE treated animals showing fatty change in individual hepatocytes in focal manner (black arrow); **Histopathological features of kidney (D)** untreated negative group of rats show normal structure of the glomeruli and tubules at the renal cortex tissue; **(E)** perivascular inflammatory cells infiltration (green arrow), oedema associated (black arrow) with degeneration in the tubular lining at the cortex (yellow arrow) of CCL4 treated animals group; **(F)** degenerative changes of some cell lining epithelium of the tubules at the cortex in CEONE treated animals.

Correspondingly, an earlier study stated that CEO-treated kidney rats showed lobulated renal corpuscles and the desquamation of the epithelial cells of the renal tubules (Shalaby *et al.* 2011). Histopathology of spleen tissues revealed atrophy and depletion were detected in the lymphoid cells of white pulps associated with congestion in the red pulps (Figure 7B). On the other hand, only congestion was detected in the red pulps and sinusoids in the spleen of CEONE-treated animals (Figure 7D), this could be attributed to the long duration of CEONE exposure, indicating non-harmful effects.

Histopathological features of the spleen: In Figure (8A) untreated control group of rats showed the normal histopathological structure of the lymphoid cells at the white pulps and the red ones as well as sinusoids were recorded. In Figure (8B) CCL4 treated animals group, atrophy, and depletion were detected in the lymphoid cells of white pulps associated (black arrow) with congestion in the red pulps (green arrow) and sub capsular oedema. In (8D) congestion



was detected in the red pulps and sinusoids in the spleen of CEONE-treated animals.

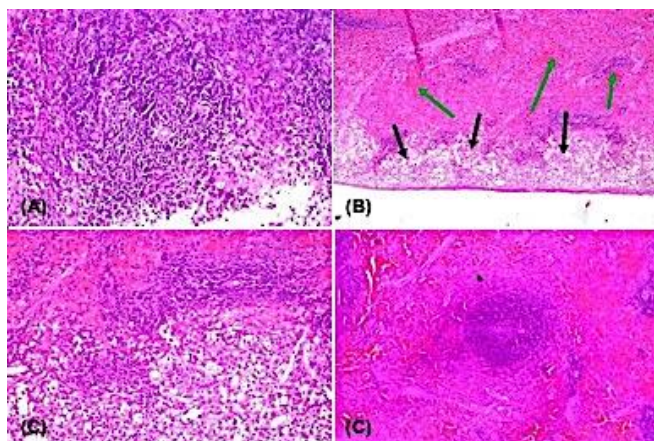


Figure 8. Histopathological features of spleen (A) untreated control group of rats showed normal histopathological structure of the lymphoid cells at the white pulps and the red one as well as sinusoids were recorded; (B) in CCL4 treated animals group, atrophy and depletion were detected in the lymphoid cells of white pulps associated (black arrow) with congestion in the red pulps (green arrow) and sub capsular oedema; (D) congestion was detected in the red pulps and sinusoids in spleen of CEONE treated animals.

Conclusion: The successful preparation of both CEONE system has been achieved by the processes of homogenization and probe sonication. The findings demonstrated that the dose-dependent inhibitory effect of CEONE and CEO on the *FOL* in laboratory and greenhouses trials was seen. It was shown that the highest level of antifungal activity was exhibited by CEONE compared to bulk CEO form at a concentration of 200 μ L. In addition, the current study did not demonstrate any remarkable histopathological effects of CEONE on liver, kidney and spleen structure, except was fatty change in individual hepatocytes in focal manner degenerative changes of some cell lining epithelium of the tubules at the cortex livers and kidneys of treated rats. But it is necessary to establish procedures for testing the oxidative potential of manufactured CEONE prior to their commercialization. Identifying the major cellular targets for NP-induced ROS will facilitate safer design and manufacture of CEONE in the market place. Therefore, we conclude that CEONE is a safe alternative to chemical fungicide as evidenced by in vitro and in vivo results. Furthermore, this study should be expanded to investigate the potential combination between CEONE and other essential oils in a synergistic formulation to enhance its activity against *FOL*.

Authors Contributions: Conceptualization, E.S.E., A.F.H. and N.A.S.M; methodology, N.A.S.M, A.F.H and A.A.A; software, A.M.I and E.S.E; validation, A.M.I and E.S.E.; formal analysis, E.S.E, N.A.S.M; investigation, A.A.A, E.Y.K; resources, A.M.I and N.A.S.M; data curation, E.S.E; writing—original draft preparation, E.S.E., A.F.H. and A.M.I; writing—review and editing, A.M.I; visualization, A.A.A, A.M.I; supervision, A.M.I; project administration, A.M.I; funding acquisition, A.M.I. All authors have read and agreed to the published version of the manuscript."

Funding: This research was kindly funded by the Deanship of Scientific Research, Vice Presidency for Graduate Studies and Scientific Research, King Faisal University, Saudi Arabia, grant number (KFU241639).

Acknowledgment: Authors extend their gratitude to the Deanship of Scientific Research, Vice Presidency for Graduate Studies and Scientific Research, King Faisal University, Saudi Arabia, for supporting the current research through grant number KFU241639.

Conflict of Interest: The authors declare no conflict of interest.

Ethical approval: All procedures carried out in studies involving animals adhered to the ethical standards of the conducting institution or practice (BUFVTM 03-01-23).

Availability of data and material: We declare that the submitted manuscript is our work, which has not been published before and is not currently being considered for publication elsewhere.

Informed consent: N/A

Consent to participate: All authors are participating in this research study.

Consent for publication: All authors are giving their consent to publish this research article in JGIAS.

SDGs addressed: Zero Hunger, Good Health, and Well-being.

REFERENCES

Abd-Elsalam, K.A. and A.R. Khokhlov. 2015. Eugenol oil nanoemulsion: antifungal activity against *Fusarium oxysporum* f. sp. *vasinfectum* and phytotoxicity on cottonseeds. Applied Nanoscience 5:255-265.

Abdulkadir, H.K., E.J. Ekefan and V.I. Gwa. 2023. Pathogenicity of *Fusarium oxysporum* f. sp. *lycopersici* (Sacc.) isolates in causing tomato wilt disease on two tomato (*Solanum lycopersicum* L) varieties. Bio-Science Research Bulletin 39:60-68.

Achore, D.S., S. Nemec and R.A. Baker. 1993. Effects of *Fusarium solani* naphthazarin toxins on the cytology and



ultra-structure of rough lemon seedlings. *Mycopathologia* 123:117-126.

Afifi, M.M.I. A.M. Ismail, S.M. Kamel and T.A Essa. 2017. Humic substances: a powerful tool for controlling *Fusarium* wilt disease and improving the growth of cucumber plants. *Journal of Plant Pathology* 99:61-67.

Ahmed, A., M. Mahmoud, M. Ouf and E. El-Fathaah. 2011. Aminoguanidine potentiates the hepatoprotective effect of silymarin in CCL4 treated rats. *Analysis of Hepatology* 10:207-215.

Ali, I.H. A.M. Elkashlan, M.A. Hammad and M. Hamdi. 2023. Antimicrobial and anti-sars-cov-2 activities of smart daclatasvir-chitosan/gelatin nanoparticles-in-*pla* nanofibrous medical textiles; *in vitro*, and *in vivo* study. *International Journal of Biological Macromolecules* 253:127350.

Ali, I.H., I.A. Khalil and I.M. El-Sherbiny. 2016. Single-dose electrospun nanoparticles-in-nanofibers wound dressings with enhanced epithelialization, collagen deposition, and granulation properties. *ACS Applied Materials and Interfaces* 8:14453-14469.

Almaghasla M.I. S.M. El-Ganainy and A.M. Ismail. 2023. Biological activity of four *Trichoderma* species confers protection against *Rhizoctonia solani*, the causal agent of cucumber damping-off and root rot diseases. *Sustainability* 15:7250.

Amini, J. and D. Sidovich. 2010. The effects of fungicides on *Fusarium oxysporum* f. sp. *lycopersici* associated with *Fusarium* wilt of tomato. *Journal of Plant Protection Research* 50:172-178.

Angioni, A., A. Barra, V. Coroneo, S. Densi and P. Cabras. 2006. Chemical composition, seasonal variability, and antifungal activity of *Lavandula stoechas* L. ssp. *Stoechas* essential oils from stem/leaves and flowers. *Journal of Agricultural and Food Chemistry* 54:4364-4370.

Anjali, C. Y. Sharma, A. Mukherjee and N. Chandrasekaran. 2012. Neem oil (*Azadirachta indica*) nanoemulsion-a potent larvical agent against *Culex Quinquefasciatus*. *Pest Management Science* 68:158-163.

Anjum, R., S.T. Sahi and I.A. Khan. 2016. Histopathological changes in response to *Ceratocystis manginecans* in mango (*Mangifera indica*). *Pakistan Journal of Agricultural Sciences* 53(1):195-199.

Aravena, R., X. Besoain, N. Riquelme, A. Salinas, M. Valenzuela, E. Oyanedel, W. Barros, Y. Olguin, A. Madrid, M. Alvear and I. Montenegro. 2021. Antifungal nanoformulation for biocontrol of tomato root and crown rot caused by *Fusarium oxysporum* f. sp. *radicis-lycopersici*. *Antibiotics* 10:1132.

Arnon, D.I. 1949. Copper enzymes in isolated chloroplasts, polyphenol oxidase in *Beta vulgaris*. *Plant Physiology* 24: 1-15.

Attia, M.S., A.M. Abdelaziz, M.M. Hassanin, A.A. Al-Askar, S.A. Marey, H. Abdelgawad and A.H Hashem. 2023. Eco-friendly preparation of thyme essential oil nano emulsion: Characterization, antifungal activity and resistance of *Fusarium* wilt disease of *Foeniculum vulgare*. *Notulae Botanicae Horti Agrobotanici Cluj-Napoca* 51:13312-13312.

Aydin, S. 2015. A short history, principles, and types of ELISA, and our laboratory experience with peptide/protein analyses using ELISA. *Peptides* 72:4-15.

Bancroft, J.D. 2002. Gamble, M. *Theory and practice of histological techniques*; Churchill Livingstone: London, UK; New York, NY, USA.

Bartucca M.L. M. Guiducci B. Falcinelli D. Del Buono P. Benincasa 2020. Blue:red LED light proportion affects vegetative parameters, pigment content, and oxidative status of einkorn (*Triticum monococcum* L. ssp. *Monococcum*) wheatgrass. *Journal of Agricultural and Food Chemistry* 68:8757-8763.

Bawa, I. 2016. Management strategies of *Fusarium* wilt disease of tomato incited by *Fusarium oxysporum* f. sp. *lycopersici* (Sacc). A review. *International Journal of Advanced Academic Research* 2:32-42.

Beckman, C.H. 1987. The nature of wilt diseases of plants. St. Paul, MN. The American Phytopathological Society. APS Press. pp. 175.

Beckman, C.H. and E. Roberts. 1995. On the nature and genetic basis for resistance and tolerance to fungal wilt diseases of plants. *Advances in Botanical Research*. 21:35-77.

Bergmeyer, H.U., G.N. Bowers Jr, M. Hørder and D.W. Moss. 1977. Provisional recommendations on IFCC methods for the measurement of catalytic concentrations of enzymes. *Clinical chemistry* 23:887-899.

Bloom, J.C. 1993. Principles of hematotoxicology: laboratory assessment and interpretation of data. *Toxicologic Pathology* 21:130-134.

Božović, M., S. Garzoli, M. Sabatino, F. Pepi, A. Baldisserotto, E. C. AndreottiRomagnoli, A. Mai, S. Manfredini and R. Rago. 2017. Essential oil extraction, chemical analysis and anti-Candida activity of *Calamintha nepeta* (L.) Savi subsp. *glandulosa* (Req.) Ball-New Approaches. *Molecules* 22 (2):203.

Brewer, M. 2011. Natural antioxidants: Sources, compounds, mechanisms of action, and potential applications. *Comprehensive Reviews in Food Science and Food Safety* 10:221-247.

Camele, I., D. Gruľová and H.S. Elshafie. 2021. Chemical composition and antimicrobial properties of *Mentha × piperita* cv. 'Kristinka' essential oil. *Plants* 10:1567.

Castillo-Sanmiguel, P.A., L.R. Cortés-Sánchez and J. Acerogodoy. 2022. Molecular aspects of tomato (*Solanum lycopersicum*) vascular wilt by *Fusarium oxysporum* f.



sp. *lycopersici* and antagonism by *Trichoderma* spp. Revista Mexicana de Fitopatología 40:82-102.

Delan, W.K. I.H. Ali, M. Zakaria, B. Elsaadany, A.R. Fares, A.N. ElMeshad and W. Mamdouh. 2022. Investigating the bone regeneration activity of PVA nanofibers scaffolds loaded with simvastatin/chitosan nanoparticles in an induced bone defect rabbit model. International Journal of Biological Macromolecules 222:2399-2413.

de Lamo, F.J. and F.L.W. Takken. 2020. Biocontrol by *Fusarium oxysporum* using endophyte-mediated resistance. Frontiers in Plant Science 11:1-15.

Dellaporta S.L. J. Wood and J.B. Hicks. 1983. A Plant DNA Minipreparation: Version II. Plant Molecular Biology Reporter 1:19-21.

Dosoky, N.S. and W.N. Setzer. 2018. Chemical composition and biological activities of essential oils of *Curcuma* species. Nutrients 10:1196.

EL Sayed, H.E., L.E., Morsy, T.M. Abo Emara and R.A. Galhom. 2019. Effect of carbon tetrachloride (CCl₄) on liver in adult albino rats: histological study. The Egyptian Journal of Hospital Medicine 76:4254-4261.

El-Beltagi, H.S., K.A. El-Naqma, M.I. Al-Daej, M.M. El-Afry, W.F. Shehata, M.F. El-Nady, A.M. Ismail, W.F. Eltonoby, A.A. Rezk and M.M.S. Metwaly. 2024. Effects of zinc nanoparticles and proline on growth, physiological and yield characteristics of pea (*Pisum sativum* L.) irrigated with diluted seawater. Cogent Food & Agriculture 10:2348695.

El-Maati, M.F., S.A. Mahgoub and S.M. Labib. 2021. Phenolic extracts of clove (*Syzygium aromaticum*) with novel antioxidant and antibacterial activities. European Journal of Integrative Medicine 8:494-504.

Enespa D.S.K. 2014. Effectiveness of some antagonistic fungi and botanicals against *Fusarium solani* and *Fusarium oxysporum* f. sp. *lycopersici* infecting Brinjal and tomato plants. Asian Journal of Plant Pathology 8:18-25.

Erel O. 2004. A novel automated method to measure total antioxidant response against potent free radical reactions. Clinical Biochemistry 37:112-9.

Fukao, T., T. Hosono, S. Misawa, T. Seki and T. Ariga. 2004. Chemoprotective effect diallyl trisulfide from garlic against carbon tetrachloride-induced acute liver injury of rats. Biofactors 21:171- 74.

Gao, H., Y. Hui and W. Chuang. 2017. Controllable preparation and mechanism of nano silver mediated by the microemulsion system of the clove oil. Results in Physics 7:1330-1336.

Ghabraie, M., K.D. Vu, L. Tata, S. Salmieri, M. Lacroix. 2016. Antimicrobial effect of essential oils in combinations against five bacteria and their effect on sensorial quality of ground meat. LWT-Food Science and Technology 66:332-339.

Ghosh, V., S. Saranya, A. Mukherjee and N. Chandrasekaran. 2013. Cinnamon oil nanoemulsion formulation by ultrasonic emulsification: investigation of its bactericidal activity. Journal of Nanoscience and Nanotechnology 13:114-122.

Gomez, K.A. and A.A. Gomez. 1984. Statistical Procedures for Agriculture Research, 2nd ed.; John Wiley: New York, NY, USA, pp.680.

Gulotta, A., A.H. Saberi, M.C. Nicoli and D.J. McClements. 2014. Nanoemulsion-based delivery systems for polyunsaturated (ω -3) oils: Formation using a spontaneous emulsification method. Journal of Agricultural and Food Chemistry 62:1720-1725.

Hamini-Kadar, N., F. Hamdane, R. Boutoutaou, M. Kihal and J.E. Henni. 2014. Antifungal activity of clove (*Syzygium aromaticum* L.) essential oil against phytopathogenic fungi of tomato (*Solanum lycopersicum* L.) in Algeria. Journal of Experimental Biology and Agricultural Sciences 2:447-454.

Hashem, A.H., A.M. AbdElaziz, M.M. Hassanin, A.A. Al-Askar, H. AbdElgawad and M.S. Attia. 2023. Potential impacts of clove essential oil nanoemulsion as bio fungicides against *Neoscytalidium* blight disease of *Carum carvi* L. Agronomy 13:1114.

Hassan, H.A. 2020. Biology and integrated control of tomato wilt caused by *Fusarium oxysporum lycopersici*: a comprehensive review under the light of recent advancements. Journal of Botany Research 3:84-99.

He, S. X. Ren, Y. Lu, Y. Zhang, Y. Wang and L. Sun. 2016. Microemulsification of clove essential oil improves its in vitro and in vivo control of *Penicillium digitatum*. Food Control 65:106-111.

Heurtault, B., P. Saulnier, B. Pech, J.E. and J.P. Proust. 2003. Benoit. Physico-chemical stability of colloidal lipid particles. Biomaterials 24:4283-4300.

Heydari, M. A. Amirjani, M. Bagheri, I. Sharifian and Q. 2020. Sabahi eco-friendly pesticide based on peppermint oil nanoemulsion: preparation, physicochemical properties, and its aphicidal activity against cotton aphid. Environmental Science and Pollution Research 27:6667-6679.

Hoeller S. A. Sperge and C. Valenta. 2009. Lecithin based nanoemulsions: A comparative study of the influence of non-ionic surfactants and the cationic phytosphingosine on physicochemical behavior and skin permeation. International Journal of Pharmaceutics 370:181-186.

Honary, S. and F. Zahir. 2013. Effect of zeta potential on the properties of nano-drug delivery systems-a review (Part 2). Tropical Journal of Pharmaceutical Research 12:265-273.

Isaac, M.R. S.G. Leyva-Mir, J. Sahagun-Castellanos, K. Camara-Correia, J.M. Tovar-Pedraza and J.E. Rodriguez-Perez. 2018. Occurrence, identification, and pathogenicity of *Fusarium* spp. associated with tomato wilt in Mexico. Notulae Botanicae Horti Agrobotanici Cluj-Napoca 46:484-493.



Ismail, A. and M. Afifi. 2019. 'Efficacy of some biotic and abiotic factors in controlling common bean rust disease caused by *Uromyces appendiculatus*', Egyptian Journal of Phytopathology 47:313-329.

Ismail, A.M. 2021. Efficacy of copper oxide and magnesium oxide nanoparticles on controlling black scurf disease on potato. Egyptian Journal of Phytopathology 49:116-130.

Ismail, A.M. and E.M. Abd El-Gawad. 2021. Antifungal activity of MgO and ZnO nanoparticles against powdery mildew of pepper under greenhouse conditions. Egyptian Journal of Agricultural Research 99:421-434.

Issac A., G. Gopakumar, R. Kuttan B. Maliakel and I.M. Krishnakumar. 2015. Safety and anti-ulcerogenic activity of a novel polyphenol-rich extract of clove buds (*Syzygium aromaticum* L.). Food and Function 6:842-852.

Jaffé, M. 1886. Ueber den niederschlag, welchen pikrinsäure in normalem harn erzeugt und über eine neue reaction des kreatinins. Biological Chemistry 10:391-400.

Joshi, M., R. Srivastava, A.K. Sharma and A. Prakash. 2013. Isolation and characterization of *Fusarium oxysporum*, a wilt causing fungus, for its pathogenic and non-pathogenic nature in tomato (*Solanum lycopersicum*). Journal of Applied and Natural Science 5:108-117.

Kar, M. and D. Mishra. 1976. Catalase, peroxidase, and polyphenoloxidase activities during rice leaf senescence. Plant Physiology 57:315-319.

Kaur, S., M.K. Samota, M. Choudhary, M. Choudhary, A.K. Pandey A. Sharma and J. Thakur. 2022. How do plants defend themselves against Pathogens-Biochemical mechanisms and genetic interventions. Physiology and Molecular Biology of Plants 28:485-504.

Kirk, J.T.O. and R.L. Allen 1965. Dependence of chloroplast pigment synthesis on protein synthesis: effect of actidione. Biochemical and Biophysical Research Communications 21:523-530.

Krzyśko-Łupicka, T., S. Sokół and A.A. 2020. Piekarska-stachowiak, evaluation of fungistatic activity of eight selected essential oils on four heterogeneous *Fusarium* isolates obtained from cereal grains in southern Poland. Molecules 25:292.

Kumar, P. S. Mishra, A. Kumar and A.K Sharma. 2016. Antifungal efficacy of plant essential oils against stored grain fungi of *Fusarium* spp. Journal of Food Science and Technology 53:3725-3734.

Kumar, R., A. Bhardwaj and L.P. Singh. 2024. Comparative life cycle assessment of environmental impacts and economic feasibility of tomato cultivation systems in northern plains of India. Scientific Reports 14:7084.

Lafuente, M.T., R., Sampedro, D. Vélez and P. Romero. 2023. Deficient copper availability on organoleptic and nutritional quality of tomato fruit. Plant Science 326:111537.

Ma, J.Q., J. Ding L. Zhang and C.M. Liu. 2014. Ursolic acid protects mouse liver against CCl₄-induced oxidative stress and inflammation by the MAPK/NF-κB pathway. Environmental Toxicology and Pharmacology 37:975-83.

Ma, M., P.W.J. Taylor, D. Chen, N. Vaghefi and J. Z. He. 2023. Major soilborne pathogens of field processing tomatoes and management strategies. Microorganisms 11:263.

Ma, Q., P.M. Davidson and Q. Zhong. 2016. Antimicrobial properties of microemulsions formulated with essential oils, soybean oil, and Tween 80. International Journal of Food Microbiology 226:20-25.

Makni, M., Y. Chtourou, E.M. Garoui, T. Boudawara and H. Fetoui. 2012. Carbon tetrachloride-induced nephrotoxicity and DNA damage in rats: Protective role of vanillin Human. Experimental Toxicology 31:844-852.

Maurya, S., S. Dubey R. Kumari and R. Verma. 2019. Management tactics for fusarium wilt of tomato caused by *Fusarium oxysporum* f. sp. *lycopersici* (Sacc.): a review. Management 4:1-7.

McClements, D.J. 2002. Colloidal basis of emulsion color. Current Opinion in Colloid & Interface Science 7:451-455.

Mishra, P., B.K. Tyagi, N. Chandrasekaran and A. Mukherjee. 2018. Biological nanopesticides: a greener approach towards the mosquito vector control. Environmental Science and Pollution Research 25:10151-10163.

Montgomery, H. and J. Dymock. 1961. The determination of nitrite in water: colorimetric method of nitric oxide assay. Analyst 86:414-416.

Mosa, M.A., K. Youssef, S.F. Hamed and A.F. Hashim. 2023. Antifungal activity of eco-safe nanoemulsions based on *Nigella sativa* oil against *Penicillium verrucosum* infecting maize seeds: Biochemical and physiological traits. Front Microbiol 18:1108733.

Mushtaq, A., S. Mohd A.R. WaniMalik, A. Gull, S. Ramniwas, G. Ahmad Nayik, S. Ercisli, R. Alina Marc, R. Ullah and A. Bari. 2023. recent insights into nanoemulsions: their preparation, properties and applications. Food Chemistry 18:100684.

Natarajan, S.K., J. Basivireddy, A. Ramachandran, S. Thomas, P. Ramamoorthy and Pulimood A.B. 2006. Renal damage in experimentally-induced cirrhosis in rats: role of oxygen free radicals. Hepatology 43:1248-1256.

Nazzaro, F., F. Fratianni, R. Coppola and V. Feo. 2017. Essential Oils and Antifungal Activity. Pharmaceuticals 10:86

Nelson, P.E.T., A. Toussoun and W.F. Marasas. 1983. *Fusarium* species. An Illustrated manual for identification (Pennsylvania State University press).



Nirmaladevi, D., M. Venkataramana and R. Srivastava. 2016. Molecular phylogeny, pathogenicity and toxicogenicity of *Fusarium oxysporum* f. sp. *lycopersici*. *Scientific Reports* 6:21367.

Ogata, M., M Hoshi and S. Urano. 2000. Antioxidant activity of eugenol and related monomeric and dimeric compounds. *Chemical and Pharmaceutical Bulletin* 48:1467-9.

Oliveira, C.M.D., M.G.F.D Carmo, L.M. Ferreira, M.D.S. Rocha, C.S. Diniz and N.M.B.D. Amaral. 2023. Control failures of Fusarium wilt on tomatoes and resistance of cultivars to the three races of the pathogen. *Revista Ceres* 70:82-90.

Padmanabhan, P.A. Cheema and G. Paliyath. 2016. Solanaceous fruits including tomato, eggplant, and peppers, editor(s): benjamin caballero, paul m. finglas, fidel toldrá, encyclopedia of food and health. Academic Press pp. 24-32.

Palfi, M., P. Konjevoda, K. Vrandečić and J. Čosić. 2019. Antifungal activity of essential oils on mycelial growth of *Fusarium oxysporum* and *Botrytis cinerea*. *Emirates Journal of Food and Agriculture* 31:544-554.

Patton, C. and S. R. Crouch. 1977. Determination of urea. *Analytical Chemistry* 49:464-469.

Perczak, A. D. Gwiazdowska, K. Marchwińska, K. Juś, R. Gwiazdowski and A. 2019. Waśkiewicz Antifungal activity of selected essential oils against *Fusarium culmorum* and *F. graminearum* and their secondary metabolites in wheat seeds. *Archives of Microbiology* 201:1085-1097.

Perveen, K. N.A. Bokhari, I. Siddique and S.A.I. Al-Rashid. 2018. antifungal activity of essential oil of *Commiphora molmol* oleo gum resin. *Journal of Essential Oil Bearing Plants* 21:667-673.

Pochapski, D.J., C. Carvalho dos Santos, G.W. Leite, S.H. Pulcinelli and C.V. Santilli. 2021. Zeta potential and colloidal stability predictions for inorganic nanoparticle dispersions: Effects of experimental conditions and electrokinetic models on the interpretation of results. *Langmuir* 37:13379-13389.

Rahman, M.A. H. Abdullah and M. Vanhaecke. 1999. Histopathology of susceptible and resistant *Capsicum annuum* cultivars infected with *Ralstonia solanacearum*. *Journal of Phytopathology* 147:129-40.

Ronis, M.J.J., J. Huang, V. Longo, N.M. Tindberg IngelmanSundberg and T.M. Badger. 1998. Expression and distribution of cytochrome P450 enzymes in male rat kidney: effects of ethanol, acetone and dietary conditions. *Biochemical Pharmacology* 55:123-129.

Ruiz-Larrea, M.B., A.M. Leal, M. Liza, M. Lacort and H. De Groot. 1994. Antioxidant effects of estradiol and 2-hydroxyestradiol on iron induced lipid peroxidation of rat liver microsomes. *Steroids* 59:383-388.

Sallam, N.M., A.M. Erakyand and A. Sallam. 2019. Effect of *Trichoderma* spp. on Fusarium wilt disease of tomato. *Molecular Biology Reports* 46:4463-4470.

Salvia-Trujillo, L.A. Rojas-Graü, R. Soliva-Fortuny and O. Martín-Belloso. 2013. Physicochemical characterization of lemongrass essential oil-alginate nanoemulsions: effect of ultrasound processing parameters. *Food Bioprocess Technology* 6:2439-2446.

Sarkhosh, A. B. A.I. Schaffer, A.J. Vargas, P. PalmateerLopez and A. Soleymani. 2018. In vitro evaluation of eight plant essential oils for controlling *Colletotrichum*, *Botryosphaeria*, *Fusarium* and *Phytophthora* Fruit rots of avocado, mango and papaya. *Plant Protection Science* 54:153-162.

Seth, U.K., N.K. Dadkar and U.G. Kamat. 1972. Selected topics in experimental pharmacology, 1st ed. Kothari Book Depot. Bombay.

Shalaby, S.E., M.M. El-Din, S.A. Abo-Donia M. Mettwally and Z.A. Attia. 2011. Toxicological effects of essential oils from eucalyptus *Eucalyptus globules* and clove *Eugenia caryophyllus* on albino rats. *Polish Journal of Environmental Studies* 20:429-434.

Sharifi-Rad, J., A. Sureda, G.C. Tenore, M. Daglia, M. Sharifi-Rad, M. Valussi, R. Tundis, M. Sharifi-Rad, M.R. Loizzo and A.O. Ademiluyi. R. Sharifi-Rad, S.A. Ayatoorai and M. Iriti. 2017. Biological activities of essential oils: From Plant Chemoeontology to Traditional Healing Systems. *Molecules* 22:70.

Sharma, A., N.K. Sharma, A. Srivastava, A. Kataria, S. Dubey, S. Sharma and B. Kundu. 2018. Clove and lemongrass oil based non-ionic nanoemulsion for suppressing the growth of plant pathogenic *Fusarium oxysporum* f. sp. *lycopersici*. *Industrial Crops and Products* 123:353-362.

Sharma, A., M. Kumar and S. Kaur. 2011. Modulatory effects of *Syzygium* solvent, oil and surfactant optimization. *International Journal of Pharmaceutics* 420:241-251.

Shi, J. K. Aisaki Y. Ikawa and W. Kenjiro. 1998. Evidence of Hepatocyte Apoptosis in Rat Liver after the Administration of Carbon Tetrachloride. *American Journal of Pathology* 153:2.

Singha I.M., Y. Kakoty, B.G. Unni, J. Das, and M.C. Kalita. 2016. Identification and characterization of *Fusarium* sp. using ITS and RAPD causing Fusarium wilt of tomato isolated from Assam, North East India. *Journal of Genetic Engineering and Biotechnology* 14:99-105.

Sirirat, S., W. Rungprom and S. Sawatdikorn. 2009. Antifungal activity of essential oils derived from some medicinal plants against grey mould (*Botrytis cinerea*). *Asian Journal of Food and Ag-Ind* 2:229-233.

Snell, F.D. and C.T. Snell. 1953. Colorimetric methods analysis including some turbidimetric and nephelometric methods". D. Van., Nostrand Company IVC., Toronto, New York, London 111:606-612.



Solans, C., P. Izquierdo, J. Nolla, N. Azemar and M.J. Garcia-Celma. 2005. Nano-Emulsions. *Curr. Opin. Colloid Interface Science* 10:102-110.

Song, W., L. Zhou, C. Yang, X. Cao, L. Zhang, and X. Liu. 2004. Tomato fusarium wilt and its chemical control strategies in a hydroponic system. *Crop Protection* 23:243-247.

Steinkellner, S., R. Mammerler and H. Vierheilig. 2005. Microconidia germination of the tomato pathogen *Fusarium oxysporum* in the presence of root exudates. *Journal of Plant Interactions* 1:23-30.

Srinivas, C. 2019. *Fusarium oxysporum* f. sp. *lycopersici* causal agent of vascular wilt disease of tomato: Biology to diversity—A review. *Saudi Journal of Biological Sciences* 26:1315-1324.

Tao, N., Q.O. and L. YangJia. 2014. Citral inhibits mycelial growth of *Penicillium italicum* by a membrane damage mechanism. *Food Control* 41:116-121.

Vijayasteltar, L., G.G., Nair, B., Maliakel, R. Kuttan, and I.M. Krishnakumar. 2016. Safety assessment of a standardized polyphenolic extract of clove buds: Subchronic toxicity and mutagenicity studies. *Toxicology Reports* 3:439-449.

Waudo, S.W. P.O. Owino and M. Kuria. 1995. Control of Fusarium wilt of tomatoes using soil amendments. *East African Agricultural and Forestry Journal* 60:235-245.

White, T.J. 1990. Amplification and Direct Sequencing of Fungal Ribosomal RNA Genes for Phylogenetics. In: Innis, M.A., Gelfand, D.H., Sninsky, J.J. and White, T.J., Eds., *PCR Protocols: A Guide to Methods and Applications*, Academic Press, New York, 315-322.

Wu, T., J. Li, Y. Li and H. Song. 2017. Antioxidant and hepatoprotective effect of swertiamarin on carbon tetrachloride-induced hepatotoxicity via the Nrf2/HO-1 pathway. *Cellular Physiology and Biochemistry* 41:2242-2254.

Zhang, J., Y. Tian, J. Wang, J. Ma, L. Liu, R. Islam, Y. Qi, J. Li and T. Shen. 2023. Inhibitory effect and possible mechanism of oregano and clove essential oils against *Pectobacterium carotovorum* subsp. *carotovorum* as onion soft rot in storage. *Postharvest Biology and Technology* 196:112164.

Zheng, J., T. Liu, Z. Guo, L. Zhang, L. Mao, Y. Zhang and H. Jiang. 2019. Fumigation and contact activities of 18 plant essential oils on *Villosiclava virens*, the pathogenic fungus of rice false smut. *Scientific Reports* 9:7330.

Zulfiqar, F. and M. Ashraf. 2022. Antioxidants as modulators of arsenic-induced oxidative stress tolerance in plants: An overview. *Journal of Hazardous Materials* 427:127891.

